Article

Heparin-Mediated Conformational Changes in Fibronectin Expose Vascular Endothelial Growth Factor Binding Sites

Maria Mitsi, Zhenning Hong, Catherine E. Costello, and Matthew A. Nugent

Biochemistry, **2006**, 45 (34), 10319-10328 • DOI: 10.1021/bi060974p

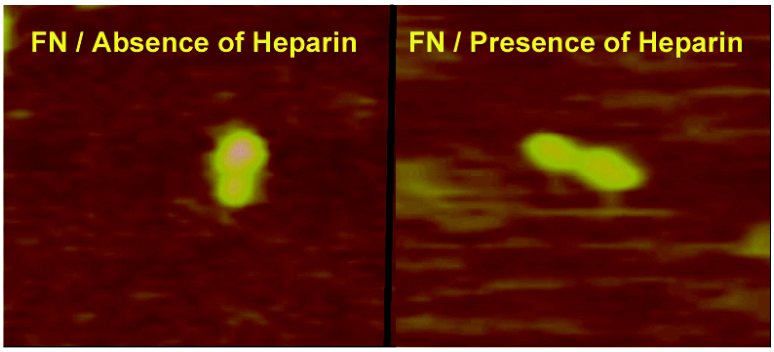

Heparin-Mediated Conformational Changes in Fibronectin Expose Vascular Endothelial Growth Factor Binding Sites†

Maria Mitsi,‡ Zhenning Hong,‡ Catherine E. Costello,‡ and Matthew A. Nugent*,‡,§,||

Departments of Biochemistry and Ophthalmology, Boston University School of Medicine, Boston, Massachusetts 02118, and Department of Biomedical Engineering, Boston University, Boston, Massachusetts 02215

Received May 17, 2006; Revised Manuscript Received June 28, 2006

ABSTRACT: Regulation of angiogenesis involves interactions between vascular endothelial growth factor (VEGF) and components of the extracellular matrix, including fibronectin and heparan sulfate. In the present study, we identified two classes of VEGF binding sites on fibronectin. One was constitutively available whereas the availability of the other was modulated by the conformational state of fibronectin. Atomic force microscopy studies revealed that heparin and hydrophilic substrates promoted the extended conformation of fibronectin, leading to increased VEGF binding. The ability of heparin to enhance VEGF binding to fibronectin was dependent on the chemical composition and chain length of heparin, since long (>22 saccharides) heparin chains with sulfation on the 6-*O* and *N* positions of glucosamine units were required for full activity. Treatment of the complex endothelial extracellular matrix with heparin also increased VEGF binding, suggesting that heparin/heparan sulfate might regulate VEGF interactions within the extracellular matrix by controlling the structure and organization of fibronectin matrices.

The extracellular matrix controls a variety of cellular functions by regulating the activity of growth factors (*1*, *2*). Fibronectin is a major component of extracellular matrices and is able to interact with a vast array of macromolecules, exhibiting a wide range of activities (*3*−*7*). Fibronectin plays important roles in angiogenesis, the process of new blood vessel formation from preexisting vessels, yet the underlying molecular mechanisms remain to be elucidated (*8*−*11*). Vascular endothelial growth factor (VEGF),[1] an endothelial cell mitogen, is a major angiogenic factor (*12*, *13*). Recent studies have shown that fibronectin contains at least two VEGF binding sites (*14*−*16*). Moreover, the interactions between fibronectin and VEGF are enhanced at acidic extracellular pH (*15*). Decreased extracellular pH, an indication of deficient vascularization, has been implicated in regulating many aspects of endothelial cell function during angiogenesis (*17*−*22*). It is possible that increased expression and deposition of VEGF under acidic conditions create a gradient of VEGF within the extracellular matrix that is used to sustain vascular growth toward hypoxic and acidic tissue regions (*23*). Binding of VEGF to fibronectin appears to be required for many of the biological activities of VEGF, including endothelial and breast cancer cell migration (*14*, *24*) and differentiation of $CD34^+$ cells to endothelial cells (*16*). In the present study, we characterized VEGF−fibronectin interactions and investigated how they are regulated by heparin and heparan sulfate, additional components of the extracellular matrix with important roles in angiogenesis (*25*−*27*). We found that heparin/heparan sulfate alter fibronectin structure exposing VEGF binding sites, thus enhancing VEGF−fibronectin interactions. Our results suggest a physical mechanism whereby heparan sulfate chains in the extracellular matrix, under appropriate stimuli, lead to the formation and/or remodeling of fibronectin-rich matrices in order to regulate VEGF angiogenic activity.

MATERIALS AND METHODS

Materials. Human recombinant $VEGF_{165}$ was obtained from R&D Systems (Minneapolis, MN) and from the NCI Bulk Cytokine and Monoclonal Antibody Preclinical Repository (Frederick, MD). ^{125}I-$VEGF_{165}$ was prepared using a modified Bolton−Hunter procedure as previously described (*23*). Heparin, desulfated derivatives, and fragments of heparin, heparan sulfate, and chondroitin sulfate were from Neoparin (San Leonardo, CA). ^{3}H-Heparin (0.413 mCi/mg) was purchased from Perkin-Elmer (Boston, MA). Heparinases I and III from *Flavobacterium heparinum* were from IBEX (Montreal, Canada). Purified human plasma fibronectin was from Chemicon International (Temecula, CA). Phosphate-buffered saline (PBS) and *N*-(2-hydroxyethyl)piperazine-*N*′-2-ethanesulfonic acid (HEPES) buffer were purchased from Invitrogen (Carlsbad, CA). Bradford protein assays were conducted using the Bio-Rad protein assay (Bio-Rad, Hercules, CA). All other reagents used were purchased from Sigma (St. Louis, MO).

† Supported by NIH Grants HL56200 and HL46902 to M.A.N. and RR10888 to C.E.C. and by a departmental grant from the Massachusetts Lions Eye Research Fund, Inc.

* To whom correspondence should be addressed at the Department of Biochemistry, Boston University School of Medicine. Tel: 617-638-4169. Fax: 617-638-5339. E-mail: mnugent@bu.edu.

‡ Department of Biochemistry, Boston University School of Medicine.

§ Department of Ophthalmology, Boston University School of Medicine.

|| Department of Biomedical Engineering, Boston University.

[1] Abbreviations: AFM, atomic force microscopy; VEGF, vascular endothelial growth factor; PlGF, placental growth factor; EGF, epidermal growth factor; FGF, fibroblast growth factor.

10.1021/bi060974p CCC: $33.50
Published on Web 08/08/2006

VEGF Binding. The 96-well hydrophobic or hydrophilic polystyrene plates (BD Falcon, number 351172, and Corning, number 3595) were coated overnight at 4 °C with human plasma fibronectin (40 nM, 6.2 pmol/cm^2) in PBS containing no Mg^{2+} or Ca^{2+} in the absence or presence of heparin. The extent of fibronectin adsorption was very similar (~50%) on both surfaces, as determined by the Bradford protein assay (*28*). Consistent with previous studies (*29*, *30*), fibronectin adsorption can be considered irreversible, since extensive incubations with NaOH/SDS solutions released only a small portion (1−2%) of the adsorbed protein. ^{125}I-VEGF$_{165}$ binding assays were conducted in 25 mM HEPES, 0.15 M NaCl, and 1 mg/mL BSA, pH 7.5 or 5.5, for 2 h at 4 °C (50 μL per well). Bound VEGF was extracted by 1 h incubation with 5 M NaCl and 25 mM HEPES, pH 7.5, followed by 1 h incubation with 1 N NaOH. The radioactivity released was measured by a Cobra Auto-Gamma 5005 counter (Packard Instruments, Meridian, CT).

Atomic Force Microscopy. Human plasma fibronectin was adsorbed overnight on hydrophobic or hydrophilic polystyrene (40 nM in PBS) or for 1 min on mica (2 nM in 10 mM ammonium acetate buffer, pH 7.0) in the absence or presence of heparin, and the surfaces were washed to remove nonadsorbed fibronectin and heparin. Tapping mode atomic force microscopy (AFM) was performed with a Digital Instruments nanoscope IIIa multimode system using silicon tips (Digital Instruments, Woodbury, NY). Atomic flat mica was purchased from Ted Pella (Redding, CA). Two types of data were collected: height mode images, where the *z*-axis position of the piezo scanner is monitored as the tip oscillates with a fixed frequency, and amplitude mode images, where the amplitude of the tip oscillation is monitored. Amplitude mode images demonstrate more clearly the edges of objects on the surface.

Roughness Analysis. The AFM images of fibronectin on polystyrene surfaces were analyzed using the Roughness Analysis commands of the Nanoscope 5.12b48 software. Prior to the analysis, the images were modified by the second-order Flatten command, which removes the Z offset between scan lines as well as the tilt and bow in each scan line, by calculating a second-order, least-squares fit for the selected segment and then subtracting it from the scan line. Subsequently, a number of roughness amplitude parameters were calculated:

(1) Root-mean-square roughness, R_q:

$$R_q = \sqrt{\frac{1}{L}\int_0^L r^2(x)\,dx} \qquad (1)$$

where $r(x)$ denotes the roughness profile, a function giving the distance from the center line of the surface profile, and L is the evaluation length over which the integral is calculated.

(2) Mean peak roughness, R_{pm}: average distance between the five highest profile points and the mean data plane.

(3) Mean valley roughness, R_{vm}: average distance between the five lowest profile points and the mean data plane.

Determination of Molecular Dimensions. The dimensions of the molecules visualized in the single-molecule AFM experiments were determined using the Section Analysis commands of the Nanoscope 5.12b48 software. The molecules we identified contained one, two, or three spherical/ellipsoid domains. We determined end-to-end distances of the whole molecules as well as heights and diameters of the individual domains. The end-to-end distances coincided, in most cases, to the overall length of the molecule due to the linear arrangement of the individual domains. Due to limitations of the software, for ellipsoid domains, we were able to determine only one diameter: the one perpendicular to the long axis of the molecule.

After the dimensions of the individual domains were obtained, the molecular volume (V_m) was calculated by treating each domain as a segment of a sphere (*31*) using the equation:

$$V_m = (h\pi/6)(3r^2 + h^2) \qquad (2)$$

where h and r denote the height and radius of the domain, respectively. On the basis of the calculated molecular volumes, the molecular mass for each individual domain was determined using the equation:

$$V_m = (M_0/N_0)(V_1 + dV_2) \qquad (3)$$

where M_0 is the molecular mass, N_0 is Avogadro's number, V_1 and V_2 are the specific volumes of the individual protein and water, respectively, and d is the extent of protein hydration. For the calculations we used standard values for V_1, V_2, and d that are accurate for most proteins: $V_1 = 0.74$ cm^3/g, $V_2 = 1$ cm^3/g, and $d = 0.4$ mol of H_2O/mol of protein (*31*).

The calculated molecular masses were very similar to the known molecular mass of a fibronectin dimer (~500 kDa), supporting the hypothesis that the observed molecule represented single fibronectin dimers. Thus, the dimensions of the ellipsoid molecules corresponded to a molecular mass of 487 ± 154 kDa, the individual domains of the two-domain category corresponded to 363 ± 63 and 152 ± 27 kDa, respectively, which sum up to 515 ± 90 kDa, and the individual domains of the three-domain category corresponded to 180 ± 57, 116 ± 45, and 128 ± 41 kDa, respectively, which give a total molecular mass of 424 ± 143 kDa.

Statistical Analysis. Comparisons of the dimensions of fibronectin molecules in the absence and in the presence of heparin were made using multivariate analysis of variance. The nonparametric Kolmogorov−Smirnov and Levene's tests suggested normal distribution and homogeneity of variance, respectively, for all of the data sets, validating the use of analysis of variance. All statistical tests were performed using the Statistical Package for the Social Sciences (SPSS) 13.0 software. The data were presented in box plots, which summarize the data using five numbers: the median, 25th and 75th percentiles, and the minimum and maximum values (not statistically outlying). The box length is the interquartile range (from 25th to 75th percentile). Outliers (values between 1.5 and 3 box lengths from the upper or lower edge of the box, denoted by circles) and extreme values (values more than 3 box lengths from the upper or lower edge of the box, denoted by stars) are also presented. On the basis of these diagrams, the outliers and extreme values were omitted from the statistical analysis.

Endothelial Cell Matrix Preparations. Bovine aortic endothelial cell matrix coated dishes were prepared as

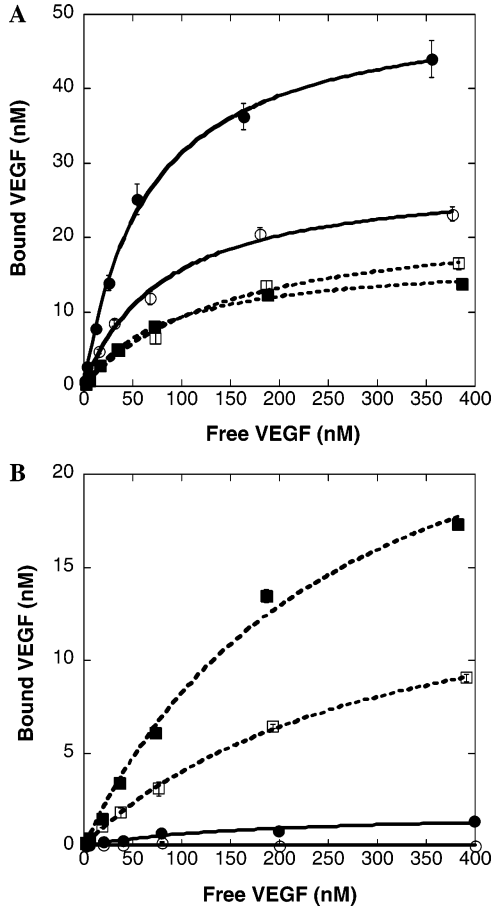

FIGURE 1: Hydrophilic (A) or hydrophobic (B) 96-well polystyrene plates were coated with human plasma fibronectin (40 nM). ^{125}I-VEGF$_{165}$ binding assays were conducted using a range of VEGF concentrations (2−400 nM) at two pH values: 7.5 (○, □) and 5.5 (●, ■). The fibronectin-bound VEGF was released with two successive incubations with 25 mM HEPES, 5 M NaCl, pH 7.5 (○, ●; solid lines), and 1 N NaOH (□, ■; dashed lines). Each data point represents the mean of quadruplicate determinations ± SE. Similar results were observed in three separate experiments.

previously described (*23*). Briefly, cells were plated into 24-well plates (effective well surface area: 2.0 cm^2) at an initial density of 5.0 × 10^4 per well, in low glucose DMEM supplemented with 10% calf serum, 100 units/mL penicillin G, and 100 μg/mL streptomycin sulfate. Six days after the cells reached confluence, the subendothelial extracellular matrix was exposed by dissolving the cell layer with 0.5% Triton and 20 mM NH_4OH in PBS at 23 °C for 3 min, followed by three washes with PBS.

RESULTS

Binding of VEGF to Fibronectin. Interactions between fibronectin and VEGF were studied with surface-immobilized fibronectin at a concentration (20 μg/mL; 40 nM) sufficient to form a monolayer (*29*, *32*). The hydrophobicity of the surface greatly affected the interactions. VEGF binding to fibronectin adsorbed on hydrophilic compared to hydrophobic polystyrene was significantly higher (Figure 1A), although the amount of adsorbed fibronectin was the same for both surfaces (data not shown). Moreover, a large fraction of bound VEGF was released by high ionic strength (60−70% of the bound VEGF was released by 5 M NaCl). On the contrary, the majority (>90%) of the VEGF bound to fibronectin adsorbed on hydrophobic polystyrene (Figure 1B) was resistant to extraction by high ionic strength and was released by NaOH, suggesting the existence of predominantly hydrophobic interactions. In addition to surface hydrophobicity, pH also affected VEGF binding to fibronectin. On the hydrophilic surface, the ionic fraction of bound VEGF increased at low pH, whereas the NaOH fraction was unaffected by pH. Increased VEGF binding at low pH was also observed on the hydrophobic surface, reflected in the NaOH fraction, which represents the predominant fraction of fibronectin-bound VEGF on this surface. The independent modulation of the two categories of bound VEGF (based on their selective extraction) indicates that they represent VEGF bound to distinct classes of binding sites. Calculation of equilibrium dissociation constant (K_d) values and number of VEGF binding sites per fibronectin dimer (Table 1), based on a simple hyperbolic model, revealed that the increase in VEGF binding observed on hydrophilic polystyrene or at low pH was the result of an increase in the number of available binding sites rather than an increase in affinity.

Table 1: Thermodynamic Parameters of VEGF−Fibronectin Interactions[a]

surface	fraction	pH	heparin	K_d (nM)	N	R
hydrophobic polystyrene	5 M NaCl	7.5	−	−[b]	–	–
			+	62 (16)	0.2 (0.02)	0.985
		5.5	−	92 (67)	0.1 (0.02)	0.906
			+	620 (470)	1.9 (0.95)	0.977
	NaOH	7.5	−	285 (58)	0.5 (0.06)	0.997
			+	79 (19)	1.0 (0.09)	0.988
		5.5	−	543 (182)	1.7 (0.38)	0.995
			+	105 (28)	1.1 (0.12)	0.988
hydrophilic polystyrene	5 M NaCl	7.5	−	91 (26)	1.7 (0.19)	0.986
			+	95 (25)	1.8 (0.18)	0.988
		5.5	−	96 (30)	3.4 (0.40)	0.985
			+	110 (22)	3.7 (0.30)	0.994
	NaOH	7.5	−	90 (25)	1.0 (0.10)	0.985
			+	79 (19)	1.0 (0.09)	0.988
		5.5	−	113 (63)	1.2 (0.27)	0.950
			+	105 (28)	1.1 (0.12)	0.988

[a] Human plasma fibronectin (40 nM) was adsorbed on hydrophobic or hydrophilic polystyrene in the absence or presence of heparin (1 μg/mL). Following adsorption ^{125}I-VEGF$_{165}$ binding assays at pH 7.5 or 5.5 were conducted as described. Fibronectin-bound VEGF was released into two successive fractions by 5 M NaCl and 1 N NaOH, respectively. K_d values and the number of binding sites per fibronectin dimer (N) were determined by fitting the experimental data presented in Figures 1 and 2 to the following hyperbolic model: [bound VEGF] = (N[free VEGF])/([free VEGF] + K_d). Nonlinear regression was performed in KaleidaGraph v3.6.2 using the Levenberg−Marquardt algorithm. In parentheses are shown the errors associated with the calculated K_d and N values. Correlation coefficient R values are also reported to show the goodness of fit. [b] There was no detectable binding under these conditions.

Heparin Modulates VEGF−Fibronectin Interactions. Adsorption of fibronectin on hydrophobic polystyrene in the presence of heparin increased the ionic fraction to a much greater extent than the NaOH fraction of bound VEGF, especially at low pH (Figure 2B,D). The increased binding resulted from a change in the number of available binding sites (Table 1). Interestingly, heparin did not affect VEGF binding to fibronectin adsorbed on hydrophilic polystyrene (Figure 2A,C). Heparan sulfate also increased VEGF binding, although to a lesser extent than heparin (Figure 3A).

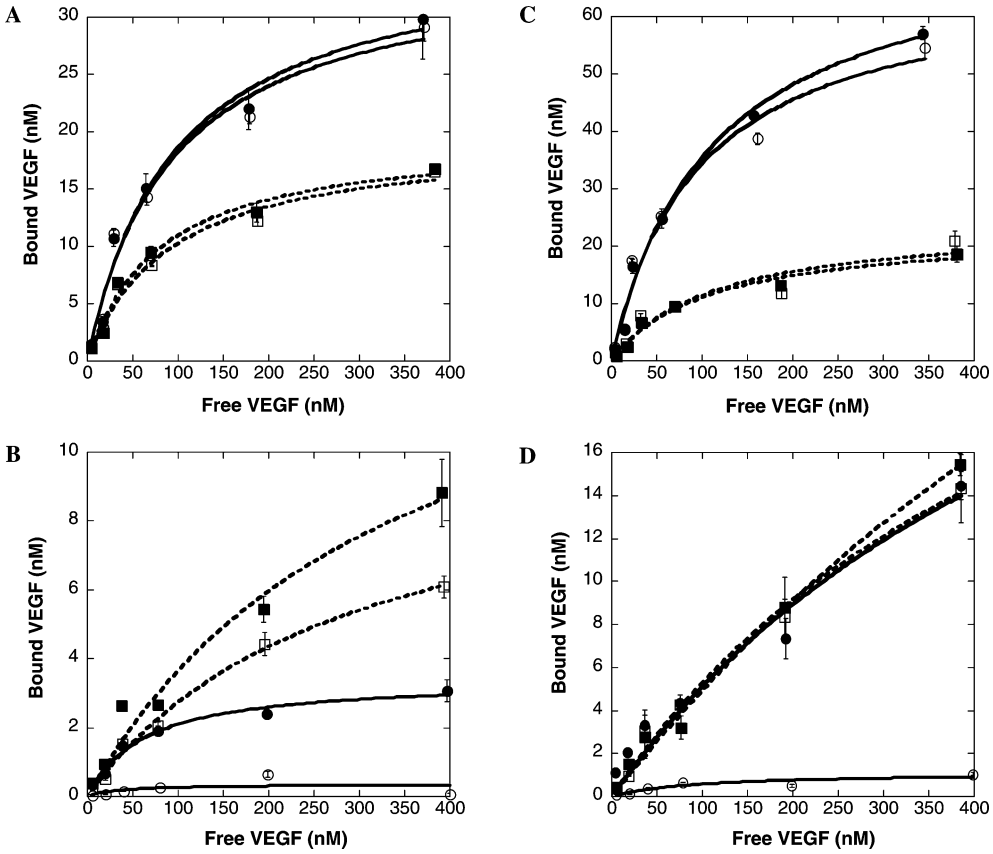

FIGURE 2: Hydrophilic (A, C) or hydrophobic (B, D) 96-well polystyrene plates were coated with human plasma fibronectin (40 nM), in the absence (○, □) or presence (●, ■) of 1 μg/mL heparin, and ^{125}I-VEGF$_{165}$ binding assays were conducted using a range of VEGF concentrations (2−400 nM) at two pH values: 7.5 (A, B) and 5.5 (C, D). The fibronectin-bound VEGF was released with two successive incubations with 25 mM HEPES, 5 M NaCl, pH 7.5 (○, ●; solid lines), and 1 N NaOH (□, ■; dashed lines). Each data point represents the mean of quadruplicate determinations ± SE.

Chondroitin sulfate and heparin fragments up to 18 saccharides in length as well as *O*- and *N*-desulfated derivatives of heparin did not affect VEGF binding. Heparin preparations with the 2-*O*- or 6-*O*-sulfate groups removed and 22 saccharide long heparin oligosaccharides enhanced binding slightly (Figure 3A,B). In addition, pretreatment of heparin and heparan sulfate with heparinase I or heparinase III, enzymes that degrade heparin and heparan sulfate, respectively, into their constituent disaccharide units, eliminated the effect on VEGF binding (data not shown). To determine if the effects of heparin on fibronectin potentially reflect an ability of heparin/heparan sulfate to modulate the interactions of VEGF with the extracellular matrix, we also conducted experiments with the endothelial deposited matrix (Figure 3C). Treatment of the endothelial matrix with heparin caused a dramatic increase in VEGF binding, while a small, statistically significant, increase in binding was also noted in matrices treated with heparan sulfate and heparin fragments containing 22 saccharides, at the highest concentration tested.

Given the fact that both fibronectin and VEGF can bind heparin, the observed effect of heparin could be explained by a mechanism whereby heparin chains bound to fibronectin can also interact with VEGF, acting as molecular bridges. However, heparin binding assays using either ^{3}H-heparin or a dimethylmethylene blue dye binding assay to measure heparin (*33*) showed that no detectable heparin was retained on the fibronectin-coated surfaces after the initial incubation and washes prior to initiating VEGF binding. This is consistent with previous observations that the binding of heparin to fibronectin is relatively weak and easily destabilized under physiological ionic strength (*34*−*36*). Thus, the ability of heparin to enhance VEGF binding to fibronectin appears to involve a stable alteration in the fibronectin matrix that is retained after heparin removal. As additional evidence that the effect of heparin on VEGF binding does not require heparin to be present after the fibronectin adsorption period, treatment of fibronectin-coated surfaces generated in the presence of heparin or heparan sulfate with heparinase I or III did not alter VEGF binding (data not shown).

To determine if the new heparin-exposed VEGF binding sites would function as general sites for other VEGF family members, we compared the abilities of VEGF$_{165}$, VEGF$_{121}$, and placental growth factor-2 (PlGF2) to compete for ^{125}I-VEGF binding to heparin-treated fibronectin matrices. Both VEGF121 and PlGF2, at the concentration tested, were as effective as VEGF$_{165}$ at competing for binding, while the unrelated factors, epidermal growth factor (EGF) and fibroblast growth factor-2 (FGF-2) were ineffective (Figure 4).

AFM Studies. To determine if the increased availability of VEGF binding sites on fibronectin adsorbed on hydrophilic polystyrene or in the presence of heparin correlated with conformational changes, the fibronectin layer was visualized by atomic force microscopy (AFM). Fibronectin adsorbed on hydrophobic polystyrene was randomly deposited on the surface, forming aggregates (Figure 5E), whereas the protein layer formed on the hydrophilic surface was more organized (Figure 5B). A similar organization of the fi-

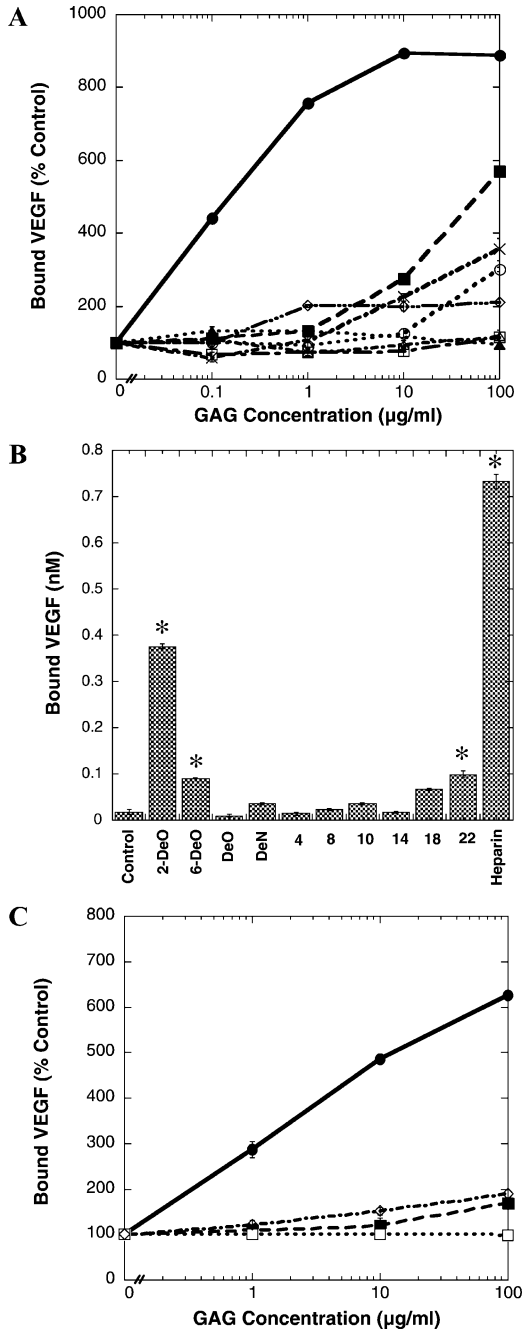

FIGURE 3: Hydrophobic 96-well polystyrene plates coated with 40 nM human plasma fibronectin (A, B) or 24-well cell culture plates coated with endothelial cell matrix (C) were treated with various glycosaminoglycans (GAGs): heparin (●), heparan sulfate (■), chondroitin sulfate (▲), 2-*O*-desulfated heparin (2-DeO) (×), in which most of the *O*-sulfate groups on C-2 of uronic acid residues have been removed, 6-*O*-desulfated heparin (6-DeO), in which most of the *O*-sulfate groups on C-6 of glucosamine residues have been removed, *O*-desulfated heparin (DeO), in which all *O*-sulfate esters of heparin have been removed, *N*-desulfated heparin (DeN) (○), in which *N*-sulfate groups of the *N*-sulfated glucosamine residues have been removed, or heparin fragments containing 4 (□), 8, 10 (△), 14, 18, or 22 (◇) saccharide units, at a range of concentrations (0.1, 1, 10, or 100 μg/mL) for (A) and (C) or at a fixed concentration (1 μg/mL) for (B). The ionic fraction of fibronectin-bound VEGF was extracted with 25 mM HEPES and 5 M NaCl, pH 7.5. For (A) and (C), the results were normalized to the control binding in the absence of any oligosaccharide. Each data point represents the mean of quadruplicate (A, B) or triplicate (C) determinations ± SE. The asterisks denote significant difference from control ($p < 0.01$) as tested by ANOVA. The ability of heparin to enhance VEGF binding to fibronectin was observed in more than 10 separate experiments.

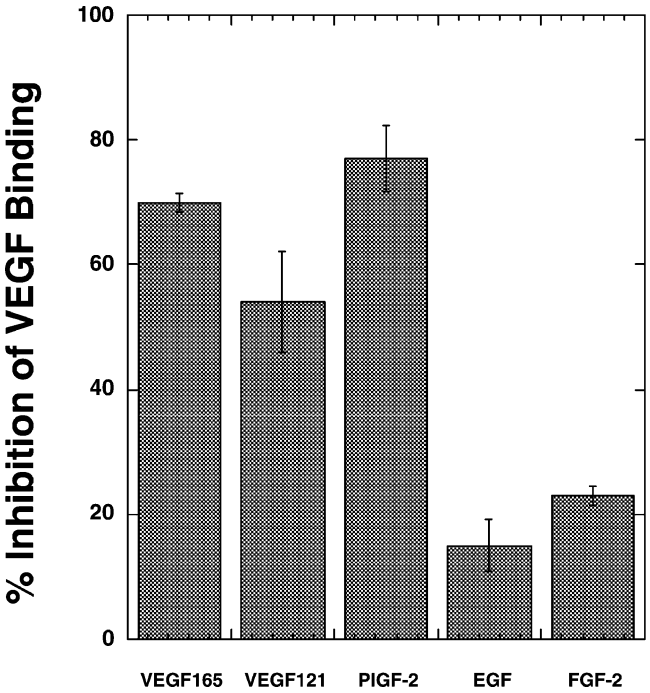

FIGURE 4: Hydrophobic 96-well polystyrene plates were coated with human plasma fibronectin (40 nM) in the presence of 1 μg/mL heparin. ^{125}I-VEGF$_{165}$ binding assays were conducted using a fixed VEGF concentration (6 nM) at pH 5.5 in the absence or presence of 10 μg/mL VEGF$_{165}$, VEGF$_{121}$, PlGF-2, EGF, or FGF-2. The ionic fraction of fibronectin-bound VEGF was released with 25 mM HEPES and 5 M NaCl, pH 7.5. The results are presented as percent inhibition of VEGF$_{165}$ binding to fibronectin in the absence of any additional growth factor. Each data point represents the mean of quadruplicate determinations ± SD.

bronectin layer was observed on the hydrophobic polystyrene when fibronectin was adsorbed in the presence of heparin (Figure 5F). Roughness measurements (Table 2) suggest that when fibronectin was adsorbed on hydrophilic surfaces or in the presence of heparin, it formed a well-organized protein layer that covered the surface in a very homogeneous way. Thus, the roughness of the surface coated with fibronectin was not significantly different than that in the absence of protein. On the contrary, adsorption of fibronectin on the hydrophobic surface in the absence of heparin caused the formation of large aggregates, increasing the roughness of the surface to a great extent (see Table 2). Single-molecule AFM measurements performed on fibronectin adsorbed on mica in the absence or presence of heparin revealed that heparin promoted an extended fibronectin conformation (Figure 6). After testing a variety of protein concentrations and buffer compositions, we concluded that 2 nM fibronectin in 10 mM ammonium acetate buffer, pH 7.0, was the optimum condition for visualization of single molecules (Figure 6A). Calculation of molecular masses, as described in the Materials and Methods section, confirmed that the molecules visualized were single fibronectin dimers and not aggregates or fragments. On both surfaces, three structural populations of fibronectin molecules were identified: compact molecules of an ellipsoid shape and molecules of a more extended configuration, containing either two or three distinct domains (Figure 6B). Seventy percent of the molecules belonged to the two-domain category, 20% of the molecules were ellipsoid, and 10% had three domains. Whereas the distribution of the molecules into the three structural popula-

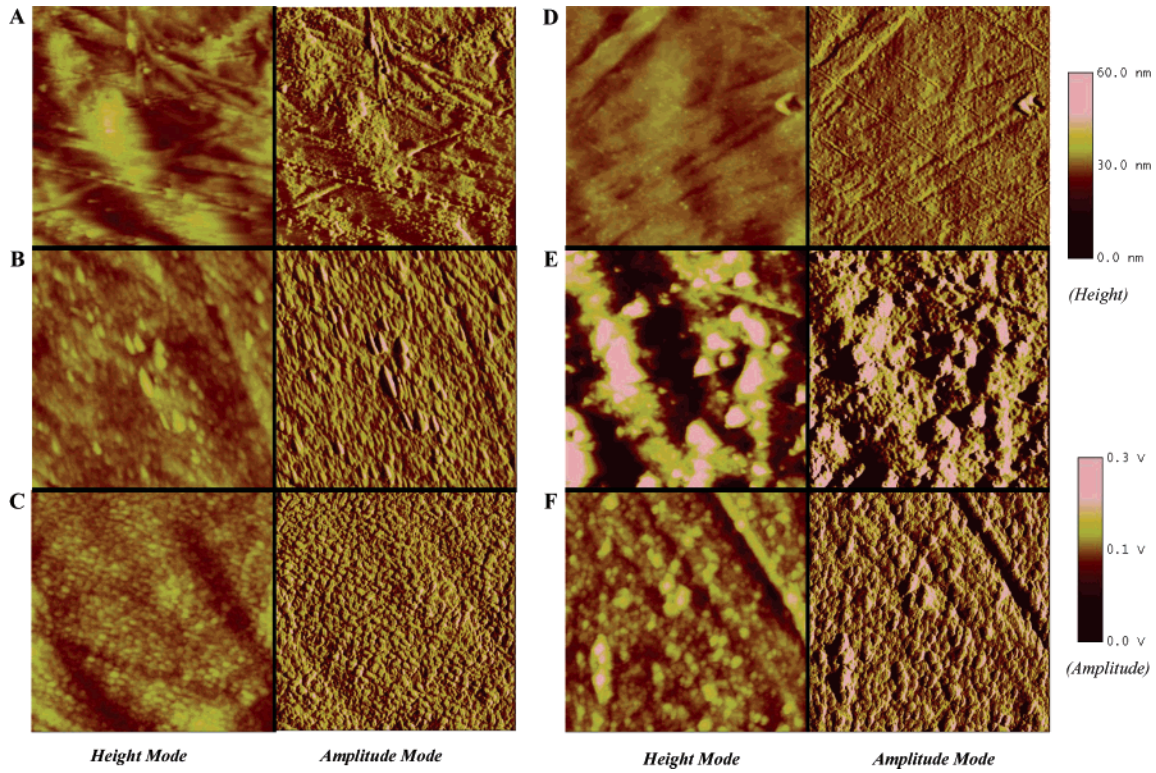

FIGURE 5: Square pieces (~1 × 1 cm^2) of hydrophilic (A−C) or hydrophobic (D−F) polystyrene were placed in 24-well plates and were incubated overnight at 4 °C with PBS (A, D) or with a solution of human plasma fibronectin (40 nM in PBS without Ca^{2+} or Mg^{2+}; 1 mL/well) in the absence (B, E) or presence (C, F) of heparin (1 μg/mL). Following fibronectin adsorption, the surface was washed extensively with H_2O, and tapping mode atomic force microscopy was performed with a Digital Instruments nanoscope IIIa multimode system using silicon tips. Polystyrene surfaces without any protein adsorbed were examined in order to determine the background image (A, D). Representative height and amplitude mode images are shown; image size = 2 × 2 μm.

Table 2: Roughness Analysis of the Polystyrene Surfaces Alone or Coated with Fibronectin in the Presence or Absence of Heparin[a]

surface	FN	heparin (μg/mL)	R_q	R_{pm}	R_{vm}	N
hydrophobic polystyrene	−	0	2.8 (1.2)	2.0 (0.4)	1.9 (0.3)	2
	+	0	9.0 (3.6)	5.2 (2.0)	4.4 (2.0)	8
	+	0.1	3.9 (0.9)	3.1 (0.4)	2.5 (0.1)	3
	+	1.0	3.7 (1.0)	2.7 (0.6)	2.3 (0.4)	11
	+	100	2.8 (0.9)	2.4 (0.1)	2.3 (0.2)	4
hydrophilic polystyrene	−	0	2.9 (1.4)	2.3 (0.7)	2.0 (0.4)	6
	+	0	3.4 (1.4)	2.3 (0.7)	2.7 (1.1)	11
	+	0.1	3.2 (1.6)	2.7 (1.0)	2.5 (0.6)	6
	+	1.0	2.6 (0.8)	2.4 (0.7)	2.7 (1.1)	8
	+	100	3.1 (1.0)	2.1 (0.4)	2.4 (0.4)	4

[a] Hydrophobic or hydrophilic polystyrene alone or coated with fibronectin (40 nM) in the absence or presence of heparin (0.1, 1, or 100 μg/mL) was analyzed by AFM as described. Roughness amplitude parameters were calculated. Root-mean-square roughness (R_q), mean peak roughness (R_{pm}), and mean valley roughness (R_{vm}) are displayed. In parentheses, the standard deviations of measurements made from N images are shown.

tions did not change with the addition of heparin, the dimensions for each individual category were different (see Supporting Information, Figure 1 and Table 1). In the absence of heparin, the domains of the molecules belonging to the two-domain category were not equivalent ($p < 0.001$); one domain was similar in dimensions with the ellipsoid molecules whereas the other was similar to the domains of the three-domain category ($p > 0.1$). Heparin increased the length of the molecules of the two-domain category with a concomitant decrease in the diameter and height of the individual domains ($p < 0.001$) such that all of the domains of the two- and three-domain categories became equivalent ($p > 0.1$). The length of the molecules of the three-domain category was increased by heparin, while the dimensions of the individual domains decreased ($p < 0.001$). Thus, heparin facilitated the separation of the individual domains.

DISCUSSION

The data presented in this study suggest a model whereby VEGF binding sites become available when fibronectin adopts its extended conformation through interactions with a hydrophilic surface or in the presence of heparin/heparan sulfate. Studies have shown that fibronectin can exist in two different conformational states, one globular and one more extended (*37*−*39*). Several factors mediate the transition from the globular to the extended form, including adsorption of fibronectin on hydrophilic surfaces (*40*). In this later case, fibronectin can sustain cell adhesion, suggesting that it adopts a conformation similar to the one found in the extracellular matrix (*32*, *41*−*43*).

We found that binding of VEGF to fibronectin adsorbed on hydrophilic polystyrene was significantly increased compared to hydrophobic polystyrene, due to an increase in the number of available binding sites, rather than through a change in affinity. We also noted that one class of VEGF binding site was available only under acidic conditions. The pH-dependent binding might be a reflection of pH-mediated conformational changes in VEGF that expose fibronectin binding sites on VEGF (unpublished data). Changes in growth factor binding to nonreceptor sites in the extracellular environment have been noted in other systems and have been

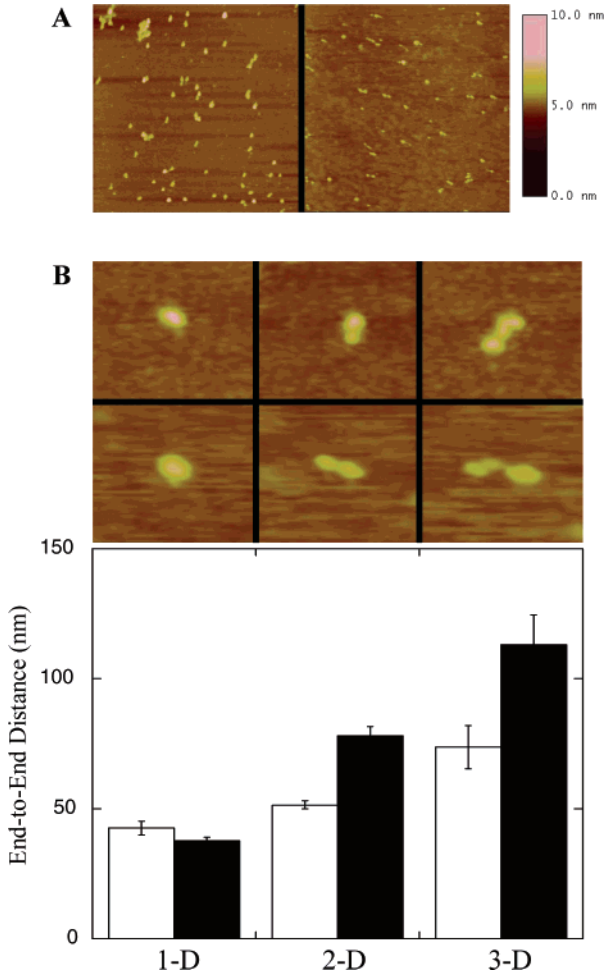

FIGURE 6: Mica surfaces were prepared by cleaving off the top layer of a piece of mica with tape. Five microliters of human plasma fibronectin (2 nM in 10 mM ammonium acetate buffer, pH 7.0) in the absence or presence of heparin (1 μg/mL) was added onto the mica and then diluted with 50 μL of H_2O on the surface. The solution was left on the surface for 1 min at room temperature. Subsequently, the surface was washed extensively with H_2O, and tapping mode atomic force microscopy was performed with a Digital Instruments nanoscope IIIa multimode system using silicon tips. (A) Representative height mode images (2 $\times$ 2 μm) of fibronectin molecules on mica in the absence (left) or presence (right) of 1 μg/mL heparin. (B) Representative molecules belonging to the three structural populations (image size 200 $\times$ 200 nm). From left to right: ellipsoid (1-D), two-domain (2-D), and three-domain (3-D) categories. Upper row: fibronectin in the absence of heparin. Lower row: fibronectin in the presence of 1 μg/mL heparin. The graph shows end-to-end distances (nm) of fibronectin molecules belonging to 1-D, 2-D, or 3-D categories in the absence (white bars) or presence (black bars) of 1 μg/mL heparin.

proposed to represent a component of biological control (*44*). The differences between the levels of VEGF binding to fibronectin on the two surfaces related to changes in fibronectin conformation, as determined by AFM. Fibronectin adsorbed on hydrophobic polystyrene formed random aggregates, whereas on the hydrophilic surface it was more organized, exhibiting significantly less roughness and covering the surface in a more homogeneous way. Fibronectin is known to contain self-association sites, which play important roles in matrix formation (*45*, *46*). When in its extended conformation, these self-association sites are exposed on the surface of the molecule, thus promoting matrix formation (*47*, *48*). Consistent with this hypothesis, the observed differences between hydrophobic and hydrophilic polystyrene might reflect the fact that fibronectin adopts its extended conformation on hydrophilic polystyrene. Interestingly, adsorption of fibronectin on hydrophobic polystyrene in the presence of heparin resulted in a similar organization of the protein layer, suggesting that heparin promotes the extended conformation of fibronectin. Indeed, analysis of single fibronectin molecules by AFM revealed that heparin mediates structural changes that lead to a more extended fibronectin conformation. It is interesting to note that once such a conformational change has occurred, the continued presence of heparin was not necessary to maintain the effect.

Results showing that VEGF binding is significantly enhanced by heparin suggest that the conformational changes mediated by heparin expose VEGF binding sites on fibronectin. While the ability of heparin and heparan sulfate to enhance protein−protein interactions by binding both proteins to create a stable ternary complex is a well-characterized mechanism for modulation of growth factor−receptor interactions (*49*, *50*), the mechanism we describe here indicates an additional function whereby heparin and heparan sulfate modulate matrix protein structure as a means to alter growth factor binding. Our analysis with other glycosaminoglycans as well as with chemical derivatives and fragments of heparin suggests that only heparin-like chains of a particular chemical composition and size are able to modulate the interactions between VEGF and fibronectin. Thus, it is possible that this process is regulated by alterations in the fine structure of the heparan sulfate synthesized by cells in response to the state of their immediate tissue environment (i.e., injury, inflammation).

Fibronectin contains at least two heparin binding sites (*34*, *35*, *51*, *52*). Binding of heparin to each of these sites is accompanied by conformational changes on the fibronectin molecule, associated with an increase in the β-sheet content of the protein (*53*−*55*), which may promote fibronectin self-association and fibrillogenesis. Moreover, several studies suggest that interaction of fibronectin with heparin leads to a partial unfolding event and/or triggers a more global structural rearrangement of fibronectin, which exposes binding sites on the surface of the molecule (*45*, *47*, *48*, *56*). Indeed, it is known that heparin stimulates fibronectin fibrillogenesis (*57*) and that cells deficient in heparan sulfate synthesis show reduced fibronectin fibrillogenesis (*58*). Thus, the exposure of VEGF binding sites that we report here is likely reflective of more general process that modulates a wide range of fibronectin−protein interactions.

It is interesting to note that treatment of the endothelial extracellular matrix caused an increase in VEGF binding in a similar fashion as observed with pure fibronectin. It is known that the extracellular matrix isolated from endothelial cell cultures (both aortic and corneal) is very rich in fibronectin (*59*, *60*). It has been reported that ~15% of the protein deposited in the endothelial cell matrix is fibronectin (*59*). It is therefore reasonable to speculate that the effect we observed reflects a heparin-induced conformational change in fibronectin within the endothelial extracellular matrix. Preliminary AFM studies of the endothelial extracellular matrix support this hypothesis (data not shown); however, it is not clear to what extent this response is attributed to fibronectin versus other components within the matrix.

The similarities in the effects of heparin on fibronectin and the more complex endothelial extracellular matrix are intriguing; however, it is important to appreciate the complexity of the extracellular matrix in interpreting these results. In this regard, our data do not rule out the possibility that heparin affects components of the matrix other than fibronectin that might mediate VEGF binding. For example, endothelial extracellular matrices also contain collagens (*61*−*63*), and it is known that collagens interact with fibronectin and heparan sulfate and can affect fibronectin matrix assembly (*64*−*66*). Collagen I fragments bind fibronectin and mediate a conformational change favoring the extended fibronectin configuration and facilitate fibronectin matrix assembly (*38*). On the other hand, recent studies have shown that the shed collagen XIII ectodomain colocalizes with fibronectin fibrils within the extracellular matrix and interferes with matrix assembly (*67*). Additional components, such as the heparan sulfate proteoglycans, perlecan, collagen XVIII, the syndecans, and their various biologically active fragments, are also likely to influence the various protein−protein and protein−heparan sulfate interactions within the extracellular matrix (*58*, *68*−*73*). Hence, attempts to fully understand fibronectin matrix remodeling within the context of the extracellular matrix will need to consider the relative interactions of all the factors present.

Our results indicate that the microenvironment within the extracellular matrix, principally the composition of heparan sulfate and pH, modulates VEGF interactions with fibronectin. These findings suggest an additional mechanism for the role of the extracellular matrix to modulate angiogenesis. Understanding the nature of interactions between angiogenic factors and extracellular matrix components will provide valuable insight into the design of new therapies aimed at stimulating or inhibiting angiogenesis to effectively treat a wide range of pathological conditions.

ACKNOWLEDGMENT

Some of the VEGF used was provided by the NCI Bulk Cytokine and Monoclonal Antibody Preclinical Repository. M.A.N. is a consultant for Momenta Pharmaceuticals, Inc.

SUPPORTING INFORMATION AVAILABLE

Statistical analysis of the dimensions of single fibronectin molecules as determined by AFM in the form of box plots (Figure 1) and molecular dimensions of fibronectin in the absence and presence of heparin (Table 1). This material is available free of charge via the Internet at http://pubs.acs.org.

REFERENCES

1. Aumailley, M., and Gayraud, B. (1998) Structure and biological activity of the extracellular matrix, *J. Mol. Med. 76*, 253−265.
2. Brownlee, C. (2002) Role of the extracellular matrix in cell-cell signalling: paracrine paradigms, *Curr. Opin. Plant Biol. 5*, 396−401.
3. Magnusson, M. K., and Mosher, D. F. (1998) Fibronectin: structure, assembly, and cardiovascular implications, *Arterioscler. Thromb. Vasc. Biol. 18*, 1363−1370.
4. Danen, E. H., and Yamada, K. M. (2001) Fibronectin, integrins, and growth control, *J. Cell. Physiol. 189*, 1−13.
5. Labat-Robert, J. (2002) Fibronectin in malignancy, *Semin. Cancer Biol. 12*, 187−195.
6. Briggs, S. L. (2005) The role of fibronectin in fibroblast migration during tissue repair, *J. Wound Care 14*, 284−287.
7. Mosher, D. F. (1989) in *Biology of Extracellular Matrix* (Mecham, R. P., Ed.) Academic Press, San Diego.
8. Clark, R. A., DellaPelle, P., Manseau, E., Lanigan, J. M., Dvorak, H. F., and Colvin, R. B. (1982) Blood vessel fibronectin increases in conjunction with endothelial cell proliferation and capillary ingrowth during wound healing, *J. Invest. Dermatol. 79*, 269−276.
9. Castellani, P., Viale, G., Dorcaratto, A., Nicolo, G., Kaczmarek, J., Querze, G., and Zardi, L. (1994) The fibronectin isoform containing the ED-B oncofetal domain: a marker of angiogenesis, *Int. J. Cancer 59*, 612−618.
10. Bloch, W., Forsberg, E., Lentini, S., Brakebusch, C., Martin, K., Krell, H. W., Weidle, U. H., Addicks, K., and Fassler, R. (1997) Beta 1 integrin is essential for teratoma growth and angiogenesis, *J. Cell Biol. 139*, 265−278.
11. George, E. L., Baldwin, H. S., and Hynes, R. O. (1997) Fibronectins are essential for heart and blood vessel morphogenesis but are dispensable for initial specification of precursor cells, *Blood 90*, 3073−3081.
12. Neufeld, G., Cohen, T., Gengrinovitch, S., and Poltorak, Z. (1999) Vascular endothelial growth factor (VEGF) and its receptors, *FASEB J. 13*, 9−22.
13. Shibuya, M. (2001) Structure and function of VEGF/VEGF-receptor system involved in angiogenesis, *Cell Struct. Funct. 26*, 25−35.
14. Wijelath, E. S., Murray, J., Rahman, S., Patel, Y., Ishida, A., Strand, K., Aziz, S., Cardona, C., Hammond, W. P., Savidge, G. F., Rafii, S., and Sobel, M. (2002) Novel vascular endothelial growth factor binding domains of fibronectin enhance vascular endothelial growth factor biological activity, *Circ. Res. 91*, 25−31.
15. Goerges, A. L., and Nugent, M. A. (2004) pH regulates vascular endothelial growth factor binding to fibronectin: a mechanism for control of extracellular matrix storage and release, *J. Biol. Chem. 279*, 2307−2315.
16. Wijelath, E. S., Rahman, S., Murray, J., Patel, Y., Savidge, G., and Sobel, M. (2004) Fibronectin promotes VEGF-induced CD34 cell differentiation into endothelial cells, *J. Vasc. Surg. 39*, 655−660.
17. Xu, L., Fukumura, D., and Jain, R. K. (2002) Acidic extracellular pH induces vascular endothelial growth factor (VEGF) in human glioblastoma cells via ERK1/2 MAPK signaling pathway: mechanism of low pH-induced VEGF, *J. Biol. Chem. 277*, 11368−11374.
18. Mousa, S. A., Lorelli, W., and Campochiaro, P. A. (1999) Role of hypoxia and extracellular matrix-integrin binding in the modulation of angiogenic growth factors secretion by retinal pigmented epithelial cells, *J. Cell. Biochem. 74*, 135−143.
19. D'Arcangelo, D., Facchiano, F., Barlucchi, L. M., Melillo, G., Illi, B., Testolin, L., Gaetano, C., and Capogrossi, M. C. (2000) Acidosis inhibits endothelial cell apoptosis and function and induces basic fibroblast growth factor and vascular endothelial growth factor expression, *Circ. Res. 86*, 312−318.
20. D'Arcangelo, D., Gaetano, C., and Capogrossi, M. C. (2002) Acidification prevents endothelial cell apoptosis by Axl activation, *Circ. Res. 91*, e4−e12.
21. Yamagata, M., Hasuda, K., Stamato, T., and Tannock, I. F. (1998) The contribution of lactic acid to acidification of tumours: studies of variant cells lacking lactate dehydrogenase, *Br. J. Cancer 77*, 1726−1731.
22. Griffiths, J. R., McIntyre, D. J., Howe, F. A., and Stubbs, M. (2001) Why are cancers acidic? A carrier-mediated diffusion model for H^+ transport in the interstitial fluid, *Novartis Found. Symp. 240*, 46−62 (discussion 62−67, 152−153).
23. Goerges, A. L., and Nugent, M. A. (2003) Regulation of vascular endothelial growth factor binding and activity by extracellular pH, *J. Biol. Chem. 278*, 19518−19525.
24. Miralem, T., Steinberg, R., Price, D., and Avraham, H. (2001) VEGF(165) requires extracellular matrix components to induce mitogenic effects and migratory response in breast cancer cells, *Oncogene 20*, 5511−5524.
25. Iozzo, R. V., and San Antonio, J. D. (2001) Heparan sulfate proteoglycans: heavy hitters in the angiogenesis arena, *J. Clin. Invest. 108*, 349−355.
26. Schonherr, E., Sunderkotter, C., Schaefer, L., Thanos, S., Grassel, S., Oldberg, A., Iozzo, R. V., Young, M. F., and Kresse, H. (2004) Decorin deficiency leads to impaired angiogenesis in injured mouse cornea, *J. Vasc. Res. 41*, 499−508.

27. Grant, D. S., Yenisey, C., Rose, R. W., Tootell, M., Santra, M., and Iozzo, R. V. (2002) Decorin suppresses tumor cell-mediated angiogenesis, *Oncogene 21*, 4765−4777.
28. Bradford, M. M. (1976) A rapid and sensitive method for the quantitation of microgram quantities of protein utilizing the principle of protein-dye binding, *Anal. Biochem. 72*, 248−254.
29. Grinnell, F., and Feld, M. K. (1981) Adsorption characteristics of plasma fibronectin in relationship to biological activity, *J. Biomed. Mater. Res. 15*, 363−381.
30. Ingber, D. E. (1990) Fibronectin controls capillary endothelial cell growth by modulating cell shape, *Proc. Natl. Acad. Sci. U.S.A. 87*, 3579−3583.
31. Schneider, S. W., Larmer, J., Henderson, R. M., and Oberleithner, H. (1998) Molecular weights of individual proteins correlate with molecular volumes measured by atomic force microscopy, *Pfluegers Arch. 435*, 362−367.
32. Kowalczynska, H. M., Nowak-Wyrzykowska, M., Dobkowski, J., Kolos, R., Kaminski, J., Makowska-Cynka, A., and Marciniak, E. (2002) Adsorption characteristics of human plasma fibronectin in relationship to cell adhesion, *J. Biomed. Mater. Res. 61*, 260−269.
33. Farndale, R. W., Buttle, D. J., and Barrett, A. J. (1986) Improved quantitation and discrimination of sulphated glycosaminoglycans by use of dimethylmethylene blue, *Biochim. Biophys. Acta 883*, 173−177.
34. Yamada, K. M., Kennedy, D. W., Kimata, K., and Pratt, R. M. (1980) Characterization of fibronectin interactions with glycosaminoglycans and identification of active proteolytic fragments, *J. Biol. Chem. 255*, 6055−6063.
35. Sekiguchi, K., Hakomori, S., Funahashi, M., Matsumoto, I., and Seno, N. (1983) Binding of fibronectin and its proteolytic fragments to glycosaminoglycans. Exposure of cryptic glycosaminoglycan-binding domains upon limited proteolysis, *J. Biol. Chem. 258*, 14359−14365.
36. Gold, L. I., Frangione, B., and Pearlstein, E. (1983) Biochemical and immunological characterization of three binding sites on human plasma fibronectin with different affinities for heparin, *Biochemistry 22*, 4113−4119.
37. Erickson, H. P., and Carrell, N. A. (1983) Fibronectin in extended and compact conformations. Electron microscopy and sedimentation analysis, *J. Biol. Chem. 258*, 14539−14544.
38. Williams, E. C., Janmey, P. A., Ferry, J. D., and Mosher, D. F. (1982) Conformational states of fibronectin. Effects of pH, ionic strength, and collagen binding, *J. Biol. Chem. 257*, 14973−14978.
39. Rocco, M., Carson, M., Hantgan, R., McDonagh, J., and Hermans, J. (1983) Dependence of the shape of the plasma fibronectin molecule on solvent composition. Ionic strength and glycerol content, *J. Biol. Chem. 258*, 14545−14549.
40. Bergkvist, M., Carlsson, J., and Oscarsson, S. (2003) Surface-dependent conformations of human plasma fibronectin adsorbed to silica, mica, and hydrophobic surfaces, studied with use of atomic force microscopy, *J. Biomed. Mater. Res. 64A*, 349−356.
41. Iuliano, D. J., Saavedra, S. S., and Truskey, G. A. (1993) Effect of the conformation and orientation of adsorbed fibronectin on endothelial cell spreading and the strength of adhesion, *J. Biomed. Mater. Res 27*, 1103−1113.
42. Burmeister, J. S., Vrany, J. D., Reichert, W. M., and Truskey, G. A. (1996) Effect of fibronectin amount and conformation on the strength of endothelial cell adhesion to HEMA/EMA copolymers, *J. Biomed. Mater. Res. 30*, 13−22.
43. Garcia, A. J., Vega, M. D., and Boettiger, D. (1999) Modulation of cell proliferation and differentiation through substrate-dependent changes in fibronectin conformation, *Mol. Biol .Cell 10*, 785−798.
44. Forsten, K. E., Akers, R. M., and San Antonio, J. D. (2001) Insulin-like growth factor (IGF) binding protein-3 regulation of IGF-I is altered in an acidic extracellular environment, *J. Cell. Physiol. 189*, 356−365.
45. Schwarzbauer, J. E. (1991) Identification of the fibronectin sequences required for assembly of a fibrillar matrix, *J. Cell Biol. 113*, 1463−1473.
46. Aguirre, K. M., McCormick, R. J., and Schwarzbauer, J. E. (1994) Fibronectin self-association is mediated by complementary sites within the amino-terminal one-third of the molecule, *J. Biol. Chem. 269*, 27863−27868.
47. Ingham, K. C., Brew, S. A., Huff, S., and Litvinovich, S. V. (1997) Cryptic self-association sites in type III modules of fibronectin, *J. Biol. Chem. 272*, 1718−1724.
48. Watanabe, K., Takahashi, H., Habu, Y., Kamiya-Kubushiro, N., Kamiya, S., Nakamura, H., Yajima, H., Ishii, T., Katayama, T., Miyazaki, K., and Fukai, F. (2000) Interaction with heparin and matrix metalloproteinase 2 cleavage expose a cryptic anti-adhesive site of fibronectin, *Biochemistry 39*, 7138−7144.
49. Nugent, M. A., and Iozzo, R. V. (2000) Fibroblast growth factor-2, *Int. J. Biochem. Cell Biol. 32*, 115−120.
50. Raman, R., Sasisekharan, V., and Sasisekharan, R. (2005) Structural insights into biological roles of protein-glycosaminoglycan interactions, *Chem. Biol. 12*, 267−277.
51. Benecky, M. J., Kolvenbach, C. G., Amrani, D. L., and Mosesson, M. W. (1988) Evidence that binding to the carboxyl-terminal heparin-binding domain (Hep II) dominates the interaction between plasma fibronectin and heparin, *Biochemistry 27*, 7565−7571.
52. Ingham, K. C., Brew, S. A., and Migliorini, M. (1994) An unusual heparin-binding peptide from the carboxy-terminal hep-2 region of fibronectin, *Arch. Biochem. Biophys. 314*, 242−246.
53. Welsh, E. J., Frangou, S. A., Morris, E. R., Rees, D. A., and Chavin, S. I. (1983) Tyrosine optical activity as a probe of the conformation and interactions of fibronectin, *Biopolymers 22*, 821−831.
54. Khan, M. Y., Jaikaria, N. S., Frenz, D. A., Villanueva, G., and Newman, S. A. (1988) Structural changes in the NH_2-terminal domain of fibronectin upon interaction with heparin. Relationship to matrix-driven translocation, *J. Biol. Chem. 263*, 11314−11318.
55. Osterlund, E., Eronen, I., Osterlund, K., and Vuento, M. (1985) Secondary structure of human plasma fibronectin: conformational change induced by calf alveolar heparan sulfates, *Biochemistry 24*, 2661−2667.
56. Bultmann, H., Santas, A. J., and Peters, D. M. (1998) Fibronectin fibrillogenesis involves the heparin II binding domain of fibronectin, *J. Biol. Chem. 273*, 2601−2609.
57. Richter, H., Wendt, C., and Hormann, H. (1985) Aggregation and fibril formation of plasma fibronectin by heparin, *Biol. Chem-.Hoppe Seyler 366*, 509−514.
58. Chung, C. Y., and Erickson, H. P. (1997) Glycosaminoglycans modulate fibronectin matrix assembly and are essential for matrix incorporation of tenascin-C, *J. Cell Sci. 110* (Part 12), 1413−1419.
59. Birdwell, C. R., Gospodarowicz, D., and Nicolson, G. L. (1978) Identification, localization, and role of fibronectin in cultured bovine endothelial cells, *Proc. Natl. Acad. Sci. U.S.A. 75*, 3273−3277.
60. Gospodarowicz, D., Greenburg, G., Vlodavsky, I., Alvarado, J., and Johnson, L. K. (1979) The identification and localization of fibronectin in cultured corneal endothelial cells: cell surface polarity and physiological implications, *Exp. Eye Res. 29*, 485−509.
61. Jaffe, E. A., Minick, C. R., Adelman, B., Becker, C. G., and Nachman, R. (1976) Synthesis of basement membrane collagen by cultured human endothelial cells, *J. Exp. Med. 144*, 209−225.
62. Kefalides, N. A. (1973) Structure and biosynthesis of basement membranes, *Int. Rev. Connect. Tissue Res. 6*, 63−104.
63. Kefalides, N. A., Cameron, J. D., Tomichek, E. A., and Yanoff, M. (1976) Biosynthesis of basement membrane collagen by rabbit corneal endothelium in vitro, *J. Biol. Chem. 251*, 730−733.
64. Di Lullo, G. A., Sweeney, S. M., Korkko, J., Ala-Kokko, L., and San Antonio, J. D. (2002) Mapping the ligand-binding sites and disease-associated mutations on the most abundant protein in the human, type I collagen, *J. Biol. Chem. 277*, 4223−4231.
65. San Antonio, J. D., Lander, A. D., Karnovsky, M. J., and Slayter, H. S. (1994) Mapping the heparin-binding sites on type I collagen monomers and fibrils, *J. Cell Biol. 125*, 1179−1188.
66. San Antonio, J. D., Slover, J., Lawler, J., Karnovsky, M. J., and Lander, A. D. (1993) Specificity in the interactions of extracellular matrix proteins with subpopulations of the glycosaminoglycan heparin, *Biochemistry 32*, 4746−4755.
67. Vaisanen, M. R., Vaisanen, T., Tu, H., Pirila, P., Sormunen, R., and Pihlajaniemi, T. (2006) The shed ectodomain of type XIII collagen associates with the fibrillar fibronectin matrix and may interfere with its assembly in vitro, *Biochem. J. 393*, 43−50.
68. Hopf, M., Gohring, W., Kohfeldt, E., Yamada, Y., and Timpl, R. (1999) Recombinant domain IV of perlecan binds to nidogens, laminin-nidogen complex, fibronectin, fibulin-2 and heparin, *Eur. J. Biochem. 259*, 917−925.
69. Hopf, M., Gohring, W., Mann, K., and Timpl, R. (2001) Mapping of binding sites for nidogens, fibulin-2, fibronectin and heparin to different IG modules of perlecan, *J. Mol. Biol. 311*, 529−541.

70. Yamagata, M., Saga, S., Kato, M., Bernfield, M., and Kimata, K. (1993) Selective distributions of proteoglycans and their ligands in pericellular matrix of cultured fibroblasts. Implications for their roles in cell-substratum adhesion, *J. Cell Sci. 106* (Part 1), 55−65.
71. Heremans, A., De Cock, B., Cassiman, J. J., Van den Berghe, H., and David, G. (1990) The core protein of the matrix-associated heparan sulfate proteoglycan binds to fibronectin, *J. Biol. Chem. 265*, 8716−8724.
72. Mongiat, M., Sweeney, S. M., San Antonio, J. D., Fu, J., and Iozzo, R. V. (2003) Endorepellin, a novel inhibitor of angiogenesis derived from the C terminus of perlecan, *J. Biol. Chem. 278*, 4238−4249.
73. Iozzo, R. V. (1998) Matrix proteoglycans: from molecular design to cellular function, *Annu. Rev. Biochem. 67*, 609−652.

BI060974P

Supplementary Fig.1. Boxplots summarizing the dimensions of fibronectin molecules in the absence (upper row) or the presence (lower row) of 1 μg/ml heparin, as determined by single-molecule AFM measurements. Molecules belong to one of three categories: ellipsoid (1-D), two-domain (2-D), three-domain (3-D). The number in parentheses (1, 2, or 3) denote the first, second and third domain of the two- and three-domain categories respectively.

The lower and upper edges of each box represent the 25^{th} and 75^{th} percentiles respectively and the line within the box marks the median. The two vertical lines outside the boxes extend to the minimum and maximum values (not statistically outlying) of the distribution. Extreme values (stars) and outliers (circles) are also presented (see *Materials and Methods*). The numbers next to the extreme values and outliers represent the actual numerical values for the points indicated. The overall lengths (end-to-end distances) of the molecules, and the diameters and heights of the individual domains are presented.

Supplementary Figure 1

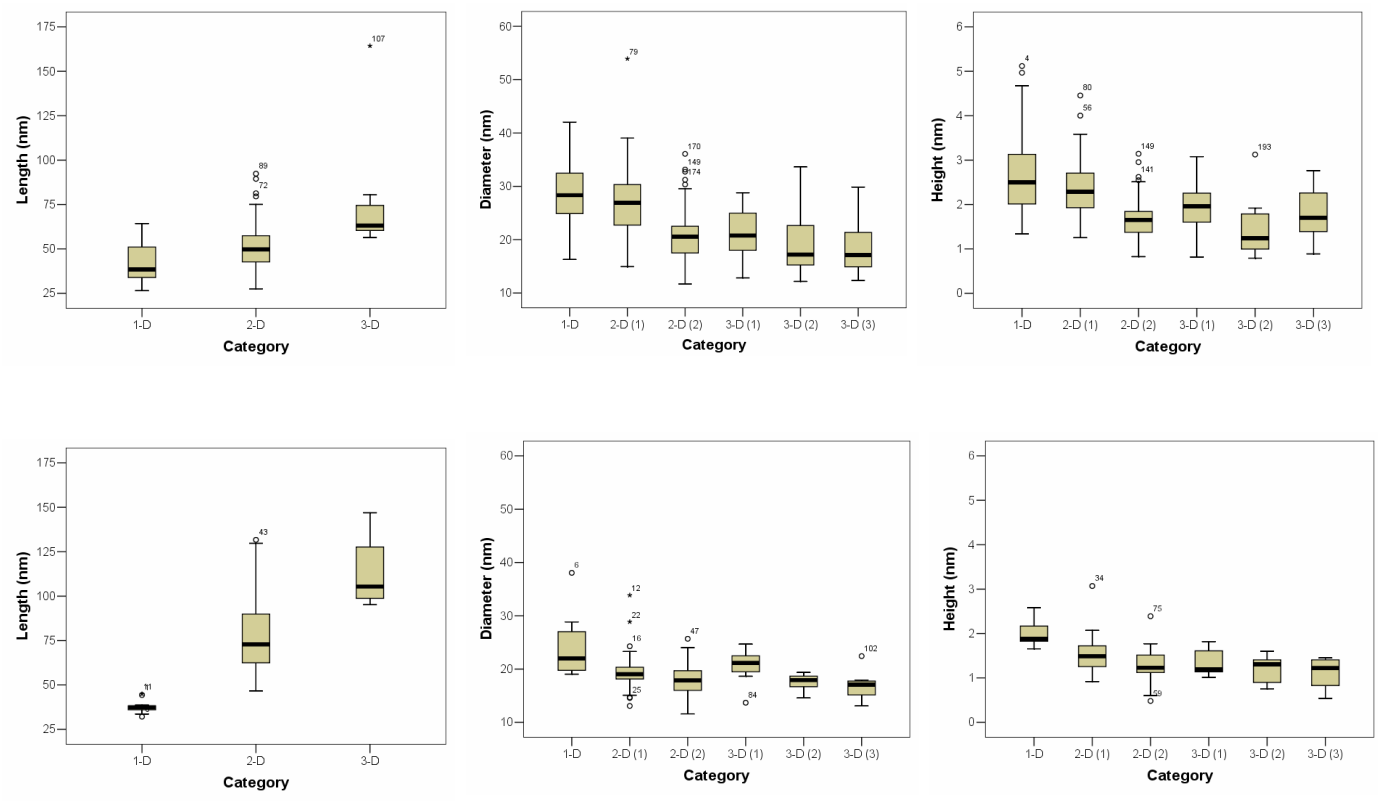

Supplementary table 1. Molecular dimensions of fibronectin dimers in the absence and presence of heparin. The dimensions of fibronectin molecules and individual domains in the absence or presence of 1 μg/ml heparin were determined by single-molecule AFM experiments as described in Fig.5. 1-D: molecules containing one domain, 2-D: molecules containing two distinct domains, 3-D: molecules containing three distinct domains. Mean values for each dimension, calculated without taking into account outliers and extreme values, as described in the statistical analysis, are presented. In parentheses, are shown standard errors of the mean. N denotes the number of molecules taken into consideration for the calculation of the mean and S.E. values for each dimension. *N equaled 7 for height and diameter measurements for the three-domain molecules in the +heparin condition. For end-to-end distance measurements in this category, N equaled 4 since only molecules with their domains aligned in a straight line could be measured.

Heparin	Domain		End-to-end distance (nm)	Diameter (nm)	Height (nm)	N
-		**1-D**	42.6 (2.8)	29.1 (1.5)	2.74 (0.25)	19
-	**2-D**	**Domain 1**	51.4 (1.5)	27.0 (0.7)	2.38 (0.07)	79
-		**Domain2**		20.8 (0.5)	1.68 (0.05)	
-	**3-D**	**Domain 1**	73.7 (8.5)	21.0 (1.5)	1.95 (0.18)	12
-		**Domain 2**		19.6 (1.9)	1.44 (0.19)	
-		**Domain 3**		18.5 (1.4)	1.78 (0.17)	
+		**1-D**	37.8 (1.2)	24.1 (1.8)	2.01 (0.09)	11
+	**2-D**	**Domain 1**	78.0 (3.6)	19.6 (0.7)	1.54 (0.07)	35
+		**Domain 2**		18.1 (0.5)	1.28 (0.06)	
+	**3-D**	**Domain 1**	113.0 (11.6)	20.5 (1.4)	1.36 (0.12)	7*
+		**Domain 2**		17.5 (0.6)	1.18 (0.13)	
+		**Domain 3**		16.9 (1.1)	1.10 (0.14)	